2763

# Chemical Behaviour of the Mixed-metal Carbonyl Clusters [Fe₂Rh(CO)₁₀]⁻ and [Fe₂Rh₂(CO)₁₂]²⁻. Crystal Structures of [Fe₂Rh(CO)₉(PPh₃)]⁻ and [Fe₂Rh₂(μ-CO)₃(CO)₉-{μ₃-Au(PPh₃)}]⁻ †

Roberto Della Pergola,*·ᵃ Lucia Fracchia,ᵃ Luigi Garlaschelli,ᵃ Mario Manassero*·ᵇ and Mirella Sansoniᵇ

ᵃ Dipartimento di Chimica Inorganica, Metallorganica ed Analitica and Centro del CNR, Università di Milano, via G. Venezian 21, 20133 Milano, Italy

ᵇ Dipartimento di Chimica Strutturale e Stereochimica Inorganica, Università di Milano, via G. Venezian 21, 20133 Milano, Italy

Addition of triphenylphosphine to the cluster [Fe₂Rh(CO)₁₀]⁻ yielded the derivative [Fe₂Rh(CO)₉(PPh₃)]⁻, which is stable enough to allow a single-crystal X-ray analysis on the [PPh₄]⁺ salt. The cluster contains a triangular metallic framework, the vertices of which are occupied by two Fe(CO)₄ groups and one Rh(CO)(PPh₃) moiety; the unsaturation of the cluster (46 valence electrons) is brought about by this 16-electron square-planar fragment. The cluster [Fe₂Rh₂(CO)₁₂]²⁻ was obtained by treating [Fe₂(CO)₈] with [Rh(CO)₄]⁻ (molar ratio 1:2) in refluxing acetone, and was characterized by infrared spectroscopy and elemental analyses. The adduct [Fe₂Rh₂(CO)₁₂-{Au(PPh₃)}]⁻ was prepared by stoichiometric addition of [Au(PPh₃)Cl] in acetone and the crystal structure of the [PPh₄]⁺ salt was elucidated by X-ray analysis. The cluster contains a trigonal-bipyramidal arrangement of metal atoms, with one Au(PPh₃) and one Fe(CO)₃ group occupying the apical positions. The vertices of the FeRh₂ equatorial plane are bound to two terminal carbonyl ligands, and the edges are spanned by three bridging carbonyls. The ³¹P NMR spectral data for [Fe₂Rh(CO)₉(PPh₃)]⁻ and [Fe₂Rh₂(CO)₁₂{Au(PPh₃)}]⁻ are consistent with the solid-state structures, but do not exclude the presence of fluxional processes in solution.

A large number of Fe–Rh[1-3] and Fe–Ir[4,5] mixed-metal unsubstituted carbonyl clusters may now be reproducibly prepared in high yields either from homometallic precursors or from preformed heterometallic species. The reactivity and stability of metal clusters from these two systems are remarkably different. For example, the tetrahedral cluster [Fe₂Ir₂(CO)₁₂]²⁻ is the most easily prepared species in the Fe–Ir family; indeed it was chosen as a precursor for a bimetallic catalyst for hydrogenation of CO.[6] In comparison, [Fe₃RhH(CO)₁₂]²⁻ was the only previously known tetrahedral Fe–Rh cluster,[3] although several tetranuclear heterometallic molecules, with different geometries or ligands other than CO, have been reported.[3,7] These observations led us to believe that the synthesis of a new Fe–Rh tetrahedral derivative was worth attempting. The two species [Fe₂Rh₂(CO)₁₂]²⁻ **1** and [Fe₂Rh₂(CO)₁₂{Au(PPh₃)}]⁻ **2** were obtained, and are described in this paper. During the course of these studies we have also re-examined the chemistry of the cluster [Fe₂Rh(CO)₁₀]⁻ **3** which has never been isolated in the solid state. The substituted derivative [Fe₂Rh(CO)₉(PPh₃)]⁻ **4** was found to be much more stable, and its crystals allowed a full structural X-ray determination.

## Results

*Synthesis of the Anions* [Fe₂Rh(CO)₁₀]⁻ *and* [Fe₂Rh-(CO)₉(PPh₃)]⁻.—Previous synthetic investigations have shown that a red anionic product is readily formed upon condensation of [{Rh(CO)₂Cl}₂] and iron carbonyl anionic
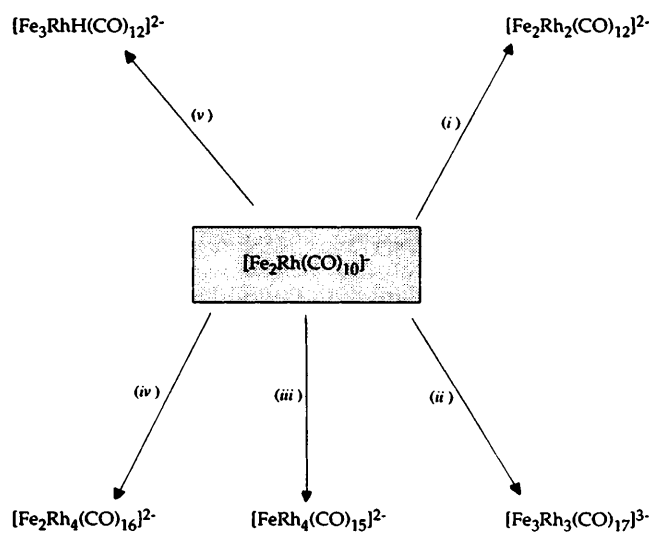
**Scheme 1** Reactivity of [Fe₂Rh(CO)₁₀]⁻. (*i*) [Rh(CO)₄]⁻; (*ii*) sodium–benzophenone; (*iii*) CO; (*iv*) propan-2-ol; (*v*) [FeH(CO)₄]⁻

complexes, such as [FeH(CO)₄]⁻ or [Fe₃(CO)₁₁]²⁻ in tetrahydrofuran (thf).[1] This mixed-metal cluster was formulated as [Fe₂Rh(CO)ₓ]⁻ (x = 10 or 11), and found to play a central role in the chemistry of the Fe–Rh system, being easily converted into several well characterized species, according to Scheme 1. However, the remarkable reactivity of the cluster hampered the isolation of the anion itself, and so its

characterization has been limited to IR and multinuclear ($^{13}$C and $^{103}$Rh) NMR spectroscopy.[1] These measurements, along with reaction (1) strongly support the presence of ten carbonyls

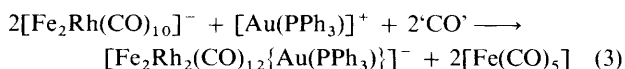$$4[FeH(CO)_4]^- + [\{Rh(CO)_2Cl\}_2] \longrightarrow$$
$$2[Fe_2Rh(CO)_{10}]^- + 2H_2 + 2Cl^- \quad (1)$$
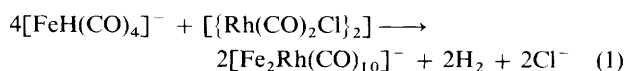
and consequently the formula $[Fe_2Rh(CO)_{10}]^-$, although the possibility of a saturated triangular cluster $[Fe_2Rh(CO)_{11}]^-$ possessing 48 c.v.e.s (cluster valence electrons) could not be definitely ruled out.[1] The preparation of $[Fe_2Rh(CO)_{10}]^-$ according to reaction (1) involves the formation of halides, which can be dissolved by propan-2-ol when the solvent is added as a precipitating agent, promoting the transformation of **3** into $[Fe_2Rh_4(CO)_{16}]^{2-}$ as depicted in Scheme 1.

The reaction of $[Fe_2(CO)_9]$ and $[Rh(CO)_4]^-$ in equimolar amounts [equation (2)], carried out at room temperature in thf,

$$[Fe_2(CO)_9] + [Rh(CO)_4]^- \longrightarrow$$
$$[Fe_2Rh(CO)_{10}]^- + 3CO \quad (2)$$
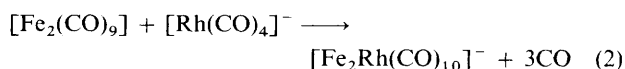
does not imply any product other than **3**, excess of CO being easily eliminated in vacuum. Several attempts were made to isolate the unsubstituted derivative by this route, but were unsuccessful. However, when a stoichiometric amount of triphenylphosphine was added, in anticipation of an addition reaction, a stable compound was formed, which could be crystallized as a $[PPh_4]^+$ salt. X-Ray analysis gave the formulation of this cluster as $[Fe_2Rh(CO)_9(PPh_3)]^-$, and showed that carbonyl substitution on the parent cluster, rather than addition, had occurred. This reaction is in keeping with those in Scheme 1, in that they are all induced by nucleophilic reagents. Reactions with electrophilic reagents also produce substantial cluster reorganization; for example the reaction of **3** with the solvated cation $[Au(PPh_3)]^+$ yields **2** and $[Fe(CO)_5]$ [equation (3)].

$$2[Fe_2Rh(CO)_{10}]^- + [Au(PPh_3)]^+ + 2^\cdot CO^\cdot \longrightarrow$$
$$[Fe_2Rh_2(CO)_{12}\{Au(PPh_3)\}]^- + 2[Fe(CO)_5] \quad (3)$$

*Synthesis of the Anions* $[Fe_2Rh_2(CO)_{12}]^{2-}$ *and* $[Fe_2Rh_2$-$(CO)_{12}\{Au(PPh_3)\}]^-$.—Several different synthetic procedures have been devised for the preparation of $[Fe_2Ir_2(CO)_{12}]^{2-}$, and the redox condensation of $[Fe_2(CO)_9]$ with $[Ir(CO)_4]^-$ was found to be the most convenient.[4] Thus, we exploited the same method for the preparation of the corresponding Fe–Rh cluster. In agreement with the greater reactivity of $[Rh(CO)_4]^-$, the reaction proceeded in acetone even at room temperature; infrared monitoring easily detected the intermediate formation of the labile cluster $[Fe_2Rh(CO)_{10}]^-$ **3**. Equations (2) and (4)

$$[Fe_2Rh(CO)_{10}]^- + [Rh(CO)_4]^- \longrightarrow$$
$$[Fe_2Rh_2(CO)_{12}]^{2-} + 2CO \quad (4)$$
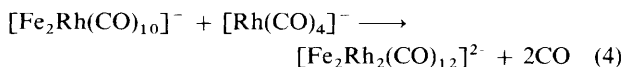
account for the formation of **1**. Both steps of this synthesis proceed at comparable rates and, within 1 h, the final product is the predominant species in solution. Complete conversion was attained by refluxing the reaction mixture for an additional hour. The $[Fe_2Rh_2(CO)_{12}]^{2-}$ cluster can be purified by pumping away the solvent in vacuum and extracting the small amount of unreacted **3** with methanol. The $[N(PPh_3)_2]^+$ and $[PPh_4]^+$ salts of **1** were produced as well shaped crystals, but found to be unsuitable for a detailed structural determination. The formula and structure were therefore inferred from the elemental analysis and the IR spectrum (see Experimental section) which is very similar to that of $[Fe_2Ir_2(CO)_{12}]^{2-}$ suggesting an analogous structure, with nine terminal and three edge-bridging CO groups.



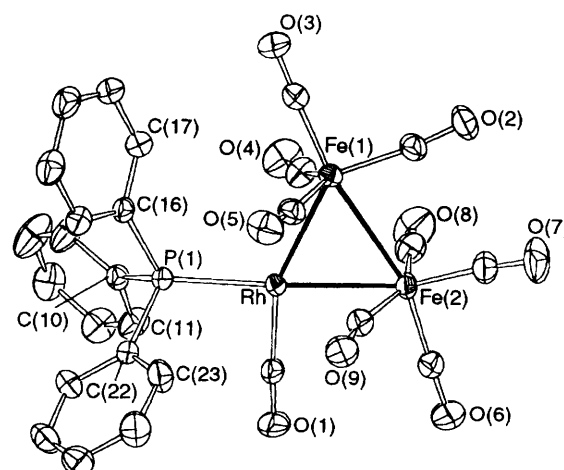**Fig. 1** An ORTEP[8] drawing of the anion $[Fe_2Rh(CO)_9(PPh_3)]^-$ with the atomic labelling scheme. Carbon atoms are numbered as the oxygen atom to which they are bound. Ellipsoids are drawn at 30% probability

It should be mentioned that the reduction of compound **3** with sodium–benzophenone selectively yielded $[Fe_3Rh_3$-$(CO)_{17}]^{3-}$.[2] The two anions $[Fe_3Rh_3(CO)_{17}]^{3-}$ and **1** have the same Fe:Rh:negative charge ratio but are obtained *via* different syntheses; the selectivity in the reduction of **3** demonstrated above is consistent with the observation that the two reaction products cannot be interconverted.

Protic acids oxidize compound **1** to $[Fe_2Rh_4(CO)_{16}]^{2-}$ and $[FeRh_5(CO)_{16}]^-$, without forming any detectable hydridic intermediate; CO induces fragmentation to $[Fe(CO)_5]$ and $[Rh(CO)_4]^-$. This behaviour is not surprising, as it was also observed for other Fe–Rh derivatives.[1] Therefore, we had to search for a substituent which could both stabilize the cluster and provide an ordered solid-state arrangement, and so we tested the $[Au(PPh_3)]^+$ group. The reaction of $[Au(PPh_3)Cl]$ and $[Fe_2Rh_2(CO)_{12}]^{2-}$ rapidly yields the expected product $[Fe_2Rh_2(CO)_{12}\{Au(PPh_3)\}]^-$, which can easily be purified and crystallized as the $[PPh_4]^+$ salt, following the same procedure used for $[Fe_2Ir_2(CO)_{12}\{Au(PPh_3)\}]^{-4}$ [equation (5)]. Excess

$$[Fe_2Rh_2(CO)_{12}]^{2-} + [Au(PPh_3)Cl] \longrightarrow$$
$$[Fe_2Rh_2(CO)_{12}\{Au(PPh_3)\}]^- + Cl^- \quad (5)$$
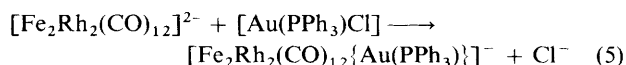
of $[Au(PPh_3)Cl]$ does not react with **2**, and we have no evidence for the addition of a second $[Au(PPh_3)]^+$ group to $[Fe_2Rh_2(CO)_{12}\{Au(PPh_3)\}]^-$.

*Solid-state Structure of* $[PPh_4][Fe_2Rh(CO)_9(PPh_3)]$ **4a**.—The anionic and cationic units are packed in the crystal lattice of compound **4a** without short contacts. The anion is shown in Fig. 1 together with the atom numbering scheme; selected bond distances and angles are in Table 1. The structure consists of a triangle of metal atoms with four CO groups bound to each Fe with the PPh$_3$ and one carbonyl ligand bound to the Rh atom. The latter CO is almost coplanar with the phosphorus and the three metal atoms. The cluster can be envisaged as being composed of two 18-electron centres, showing a distorted-octahedral co-ordination, and one 16-electron square-planar fragment, sharing pairs of electrons in localized metal–metal bonds.

The Rh–Fe distances associated with the unsaturated metal centre are anomalously short: Rh–Fe(2), *trans* to PPh$_3$ [2.619(1) Å], is slightly longer than Rh–Fe(1), *trans* to CO [2.602(1) Å]. Within this anion the Fe–Fe bond is the longest metal–metal interaction [2.782(1) Å]. The Rh–C(1) distance is 1.830(2) Å, longer than the average Fe–C distance (1.780 Å) whilst the average C–O bond length is 1.149 Å, with C(1)–O(1)

**Table 1** Selected bond distances (Å) and angles (°) for the anion $[Fe_2Rh(CO)_9(PPh_3)]^-$ **4** with estimated standard deviations (e.s.d.s) in parentheses

| | | | |
|---|---|---|---|
| Rh–Fe(1) | 2.602(1) | Fe(1)–C(4) | 1.779(2) |
| Rh–Fe(2) | 2.619(1) | Fe(1)–C(5) | 1.794(3) |
| Fe(1)–Fe(2) | 2.782(1) | Fe(2)–C(6) | 1.760(2) |
| Rh–P(1) | 2.284(1) | Fe(2)–C(7) | 1.780(3) |
| Rh–C(1) | 1.830(2) | Fe(2)–C(8) | 1.799(3) |
| Fe(1)–C(2) | 1.762(3) | Fe(2)–C(9) | 1.803(3) |
| Fe(1)–C(3) | 1.762(2) | C–O (average) | 1.149 |
| | | | |
| Fe(1)–Rh–Fe(2) | 64.38(3) | Fe(2)–C(9)–O(9) | 166.6(2) |
| Rh–Fe(1)–Fe(2) | 58.10(3) | M–C–O (average) | 173.7 |
| Fe(1)–Fe(2)–Rh | 57.52(3) | C(1)–Rh–P(1) | 91.80(9) |
| Rh–C(1)–O(1) | 176.3(2) | Fe(2)–Rh–C(1) | 93.10(8) |
| Fe(1)–C(4)–O(4) | 167.7(2) | Fe(1)–Rh–P(1) | 110.62(1) |

**Table 2** Selected bond distances (Å) and angles (°) for the anion $[Fe_2Rh_2(CO)_{12}\{Au(PPh_3)\}]^-$ **2** with e.s.d.s in parentheses (t = terminal, br = bridging)

| | | | |
|---|---|---|---|
| Au–Rh(1) | 2.782(1) | Fe(1)–C(5) | 1.786(5) |
| Au–Rh(2) | 2.781(1) | Fe(1)–C(6) | 1.759(5) |
| Au–Fe(2) | 2.793(1) | Fe(1)–C(7) | 1.790(5) |
| Rh(1)–Rh(2) | 2.732(1) | Fe(2)–C(3) | 1.824(5) |
| Rh(1)–Fe(1) | 2.634(1) | Fe(2)–C(4) | 1.805(5) |
| Rh(1)–Fe(2) | 2.750(1) | Rh(1)–C(10) | 2.143(5) |
| Rh(2)–Fe(1) | 2.640(1) | Rh(1)–C(11) | 2.127(5) |
| Rh(2)–Fe(2) | 2.760(1) | Rh(2)–C(10) | 2.015(5) |
| Fe(1)–Fe(2) | 2.656(1) | Rh(2)–C(12) | 2.105(5) |
| Au–P(1) | 2.283(2) | Fe(2)–C(11) | 1.993(5) |
| Rh(1)–C(1) | 1.894(5) | Fe(2)–C(12) | 2.042(5) |
| Rh(1)–C(2) | 1.857(5) | $C_t$–$O_t$ (average) | 1.142 |
| Rh(2)–C(8) | 1.806(6) | $C_{br}$–$O_{br}$ (average) | 1.156 |
| Rh(2)–C(9) | 1.846(5) | | |
| | | | |
| Rh(1)–C(10)–O(10) | 135.4(4) | Fe(2)–C(12)–O(12) | 140.2(5) |
| Rh(2)–C(10)–O(10) | 142.4(4) | Fe(1)–Rh(1)–C(1) | 176.3(2) |
| Rh(1)–C(11)–O(11) | 134.0(4) | Fe(1)–Rh(2)–C(9) | 175.4(2) |
| Fe(2)–C(11)–O(11) | 142.3(4) | Fe(1)–Fe(2)–C(3) | 175.8(2) |
| Rh(2)–C(12)–O(12) | 136.4(5) | M–$C_t$–$O_t$ (average) | 175.1 |



**Fig. 2** An ORTEP drawing of the anion $[Fe_2Rh_2(CO)_{12}\{Au(PPh_3)\}]^-$ with the atomic labelling scheme. Other details as in Fig. 1

being the shortest [1.138(2) Å], in keeping with smaller $\pi^*$ back donation from the rhodium(I) centre. The M–C–O angles have a mean value of 173.7°, but close inspection reveals that two CO ligands [one for each iron atom, Fe(1)–C(4)–O(4) 167.7(2) and Fe(2)–C(9)–O(9) 166.6(2)°], are slightly asymmetric, being bent towards the Rh atom with contacts of 2.432(2) and 2.431(2) Å, respectively.

*Solid-state Structure of* $[PPh_4][Fe_2Rh_2(\mu\text{-}CO)_3(CO)_9\{Au(PPh_3)\}]$ **2a**.—The crystal structure of compound **2a** consists of discrete $[PPh_4]^+$ cations and $[Fe_2Rh_2(CO)_{12}\{Au(PPh_3)\}]^-$ anions, with normal van der Waals contacts. An ORTEP[8] view of the anion is shown in Fig. 2 together with the atom numbering scheme; selected bond distances and angles are in Table 2. The metallic framework can be described as a trigonal bipyramid, with $Fe(CO)_3$ and $Au(PPh_3)$ fragments occupying the apical vertices, whilst two rhodium and the remaining iron atom are located in the equatorial positions, each being connected to only two terminal ligands. All the edges of the equatorial plane are spanned by bridging groups. Two metal

sites in the equatorial plane are affected by disorder, showing fractional occupation numbers of $Rh_{0.56}Fe_{0.44}$ for the metal atom labelled Rh(2) and $Rh_{0.44}Fe_{0.56}$ for that labelled Fe(2) (see Experimental section). This behaviour has frequently been observed in mixed-metal clusters of a $d^9$ metal and iron,[1,4,5,9] and is present to a similar extent in the corresponding $[Fe_2Ir_2(CO)_{12}\{Au(PPh_3)\}]^-$ anion. The idealized symmetry of a single anion is $C_s$, with the mirror plane passing through Fe(2), Fe(1) and bisecting the Rh–Rh bond; however, due to the disorder affecting the Rh(2) and Fe(2) sites, the arrangement of the clusters in the crystal is more consistent with a statistical mirror containing Fe(1), Rh(1) and relating Fe(2) and Rh(2).

The metal–metal bond distances in the cluster can be grouped logically into three sets: (*i*) Au–$M_{eq}$ (average 2.785 Å), (*ii*) Fe(1)–$M_{eq}$ (average 2.653 Å), and (*iii*) $M_{eq}$–$M_{eq}$ (average 2.747 Å) (eq = equatorial). Within each set, differences between Fe and Rh cannot be appreciated, due to the site disorder. The gold capping atom is connected to the cluster framework with the longest distances, the $Fe(CO)_3$ group with the shortest; the three metal–metal bond lengths of the equatorial plane are affected both by the shortening effect of edge-bridging carbonyls and the lengthening effect of the $\mu_3$-$Au(PPh_3)$ fragment, the latter being prevalent. The disorder between Fe and Rh is more evident in the M–CO distances (t = terminal, br = bridging): Fe(2)–$C_t$ and Rh(2)–$C_t$ (the sites where Fe and Rh are mixed) are longer than Fe(1)–$C_t$ and shorter than Rh(1)–$C_t$ (1.820 *vs.* 1.778 and 1.876 Å, respectively). The M–$C_{br}$ distances are equally affected, since Rh(1)–$C_{br}$ averages 2.135 Å, and the other M–$C_{br}$ 2.039 Å. The mean C–O bond length is 1.142 Å for terminal ligands and 1.156 for $\mu$–C–O; average M–C–O angles are 175.1 and 138.5°, respectively. The Au–P distance is 2.283(2) Å which is typical for such a fragment.[4,10]

## Discussion

The clusters $[Fe_2Rh_2(CO)_{12}]^{2-}$ and $[Fe_2Rh_2(CO)_{12}\{Au(PPh_3)\}]^-$ contain 60 and 72 c.v.e.s, respectively, numbers which do not deserve any special comment, since they are typical for tetrahedral and trigonal-bipyramidal metal arrangements.[11] Instead, the 46 c.v.e.s of $[Fe_2Rh(CO)_9(PPh_3)]^-$ are indicative of a co-ordinatively unsaturated metal cluster.

Triangular species containing less than 48 c.v.e.s are well documented. The best known example is $[Os_3H_2(CO)_{10}]$ (46), which contains a hydride-bridged double osmium–osmium

**Table 3** Crystallographic data

| Compound | $[PPh_4][Fe_2Rh(CO)_9(PPh_3)]$ **4a** | $[PPh_4][Fe_2Rh_2(CO)_{12}\{Au(PPh_3)\}]$ **2a** |
|---|---|---|
| Formula | $C_{51}H_{35}Fe_2O_9P_2Rh$ | $C_{54}H_{35}AuFe_2O_{12}P_2Rh_2$ |
| $M$ | 1068.4 | 1452.3 |
| Crystal system | Triclinic | Monoclinic |
| Space group | $P\bar{1}$ | $P2_1/c$ |
| $a/\text{Å}$ | 12.277(4) | 10.992(3) |
| $b/\text{Å}$ | 12.380(4) | 13.724(3) |
| $c/\text{Å}$ | 17.871(6) | 35.982(6) |
| $\alpha/°$ | 70.56(3) | |
| $\beta/°$ | 74.78(3) | 97.61(2) |
| $\gamma/°$ | 67.80(3) | |
| $U/\text{Å}^3$ | 2342(2) | 5380(2) |
| $Z$ | 2 | 4 |
| $F(000)$ | 1080 | 2824 |
| $D_c/\text{g cm}^{-3}$ | 1.515 | 1.793 |
| Crystal dimensions/mm | $0.29 \times 0.45 \times 0.50$ | $0.12 \times 0.28 \times 0.48$ |
| Colour | Dark red | Black |
| $\mu(\text{Mo-K}\alpha)/\text{cm}^{-1}$ | 10.7 | 39.5 |
| Minimum transmission factor | 0.90 | 0.66 |
| Scan mode | $\omega$ | $\omega$ |
| $\omega$-Scan width/° | $1.1 + 0.35 \tan \theta$ | $1.0 + 0.35 \tan \theta$ |
| $\theta$ range/° | 3–25 | 3–25 |
| Reciprocal space explored | $+h, \pm k, \pm l$ | $+h, +k, \pm l$ |
| Measured reflections | 8220 | 9925 |
| Unique observed reflections with $I > 3\sigma(I)$ | 6671 | 6170 |
| Final $R$ and $R'$ indices [a] | 0.023, 0.033 | 0.024, 0.026 |
| No. of variables | 586 | 658 |
| Goodness of fit [b] | 1.31 | 1.09 |

[a] $R = [\Sigma(\||F_o| - k|F_c\||)/\Sigma|F_o|]$, $R' = [\Sigma w(|F_o| - k|F_c|)^2/\Sigma w F_o^2]^{\frac{1}{2}}$. [b] $[\Sigma w(\||F_o| - k|F_c\||)^2/(N_o - N_v)]^{\frac{1}{2}}$ where $w = 1/[\sigma(F_o)]^2$, $\sigma(F_o) = [\sigma^2(I) + (iI)^2]^{\frac{1}{2}}/2F_o L_p$, $N_o$ is the number of observations, $N_v$ the number of variables, and $i$, the ignorance factor, $= 0.04$ for compound **4a** and 0.03 for **2a**.

**Table 4** Fractional atomic coordinates with e.s.d.s in parentheses for $[PPh_4][Fe_2Rh(CO)_9(PPh_3)]$ **4a**

| Atom | $x$ | $y$ | $z$ | Atom | $x$ | $y$ | $z$ |
|---|---|---|---|---|---|---|---|
| Rh | 0.373 46(1) | −0.187 39(1) | 0.289 73(1) | C(20) | 0.254 4(3) | 0.230 0(2) | 0.409 7(2) |
| Fe(1) | 0.158 56(2) | −0.071 82(2) | 0.256 27(2) | C(21) | 0.337 6(2) | 0.125 5(2) | 0.392 1(1) |
| Fe(2) | 0.321 18(3) | −0.240 47(3) | 0.176 11(2) | C(22) | 0.548 0(2) | −0.079 7(2) | 0.344 0(1) |
| P(1) | 0.409 07(4) | −0.115 55(4) | 0.380 19(3) | C(23) | 0.572 1(2) | −0.023 5(2) | 0.263 2(1) |
| P(2) | −0.049 83(5) | −0.482 99(4) | 0.177 48(3) | C(24) | 0.673 0(2) | 0.010 6(3) | 0.232 7(2) |
| O(1) | 0.618 6(2) | −0.359 8(2) | 0.273 8(1) | C(25) | 0.751 7(2) | −0.012 0(2) | 0.282 1(2) |
| O(2) | 0.011 4(2) | −0.070 6(2) | 0.151 6(1) | C(26) | 0.730 1(2) | −0.068 4(2) | 0.361 7(2) |
| O(3) | −0.045 6(2) | 0.094 4(2) | 0.330 4(1) | C(27) | 0.628 3(2) | −0.101 6(2) | 0.394 0(1) |
| O(4) | 0.157 0(2) | −0.253 3(2) | 0.411 1(1) | C(28) | −0.124 6(2) | −0.338 4(2) | 0.115 7(1) |
| O(5) | 0.268 3(2) | 0.120 4(2) | 0.189 5(1) | C(29) | −0.210 2(2) | −0.325 6(2) | 0.073 4(1) |
| O(6) | 0.531 0(2) | −0.431 7(2) | 0.131 4(1) | C(30) | −0.269 7(2) | −0.212 0(3) | 0.029 4(2) |
| O(7) | 0.220 0(2) | −0.191 3(2) | 0.032 9(1) | C(31) | −0.244 2(2) | −0.113 0(2) | 0.027 1(2) |
| O(8) | 0.227 1(2) | −0.421 5(2) | 0.301 9(2) | C(32) | −0.155 7(3) | −0.124 7(2) | 0.066 1(2) |
| O(9) | 0.453 4(2) | −0.065 7(2) | 0.108 8(1) | C(33) | −0.096 0(2) | −0.237 7(2) | 0.110 5(1) |
| C(1) | 0.525 1(2) | −0.293 5(2) | 0.282 3(1) | C(34) | −0.091 6(2) | −0.484 6(2) | 0.282 4(1) |
| C(2) | 0.075 5(2) | −0.077 0(2) | 0.191 5(2) | C(35) | −0.141 1(2) | −0.568 9(3) | 0.336 9(1) |
| C(3) | 0.035 7(2) | 0.028 7(2) | 0.302 1(1) | C(36) | −0.173 9(3) | −0.566 9(3) | 0.416 7(2) |
| C(4) | 0.170 8(2) | −0.187 6(2) | 0.347 9(1) | C(37) | −0.155 5(3) | −0.484 0(3) | 0.442 3(2) |
| C(5) | 0.232 8(2) | 0.040 1(2) | 0.213 6(1) | C(38) | −0.106 1(4) | −0.401 7(3) | 0.388 9(2) |
| C(6) | 0.448 8(2) | −0.356 3(2) | 0.149 7(1) | C(39) | −0.073 1(3) | −0.400 5(3) | 0.307 7(2) |
| C(7) | 0.255 2(2) | −0.208 7(2) | 0.090 4(1) | C(40) | −0.088 1(2) | −0.598 3(2) | 0.160 2(1) |
| C(8) | 0.259 3(2) | −0.346 9(2) | 0.254 1(2) | C(41) | −0.206 0(2) | −0.597 5(2) | 0.179 2(1) |
| C(9) | 0.398 8(2) | −0.130 9(2) | 0.143 8(1) | C(42) | −0.234 7(2) | −0.683 7(2) | 0.161 6(1) |
| C(10) | 0.429 9(2) | −0.218 1(2) | 0.480 3(1) | C(43) | −0.147 7(2) | −0.768 9(2) | 0.126 1(1) |
| C(11) | 0.505 6(3) | −0.335 1(2) | 0.487 8(1) | C(44) | −0.031 2(2) | −0.770 6(2) | 0.108 2(1) |
| C(12) | 0.527 5(3) | −0.413 3(3) | 0.562 6(2) | C(45) | 0.000 3(2) | −0.685 1(2) | 0.125 1(1) |
| C(13) | 0.472 9(3) | −0.376 6(2) | 0.630 3(2) | C(46) | 0.108 3(2) | −0.514 2(2) | 0.150 8(1) |
| C(14) | 0.397 5(4) | −0.261 5(3) | 0.624 3(2) | C(47) | 0.158 8(2) | −0.467 9(2) | 0.072 9(1) |
| C(15) | 0.375 5(3) | −0.182 7(2) | 0.549 7(2) | C(48) | 0.280 4(2) | −0.501 2(3) | 0.051 9(2) |
| C(16) | 0.303 2(2) | 0.025 7(2) | 0.402 5(1) | C(49) | 0.352 2(2) | −0.580 2(2) | 0.107 1(2) |
| C(17) | 0.184 3(2) | 0.033 8(2) | 0.431 3(1) | C(50) | 0.303 8(2) | −0.626 8(3) | 0.183 8(2) |
| C(18) | 0.102 2(2) | 0.138 5(3) | 0.448 8(2) | C(51) | 0.182 0(2) | −0.593 9(2) | 0.206 2(1) |
| C(19) | 0.137 1(3) | 0.236 6(2) | 0.438 0(2) | | | | |

bond, as confirmed by the short Os–Os distance and by its reactivity: the cluster can easily add two-electron donors and reach saturation.[12] Other typical examples are the triangular clusters containing $PtL_2$ fragments; in these derivatives up to one orbital per platinum atom lies so high in energy that it is not available for cluster bonding: the number of c.v.e.s can thus be lowered to 42.[13]

Some heterobimetallic phosphide-bridged compounds, such

**Table 5** Fractional atomic coordinates with e.s.d.s in parentheses for $[PPh_4][Fe_2Rh_2(CO)_{12}\{Au(PPh_3)\}]$ **2a**

| Atom | $x$ | $y$ | $z$ | Atom | $x$ | $y$ | $z$ |
|---|---|---|---|---|---|---|---|
| Au | 0.141 19(2) | 0.404 23(1) | 0.655 03(1) | C(19) | −0.055 6(4) | 0.466 9(3) | 0.717 7(1) |
| Rh(1) | 0.131 85(3) | 0.342 26(3) | 0.581 09(1) | C(20) | −0.072 2(4) | 0.475 4(4) | 0.754 7(1) |
| Rh(2) | 0.130 00(4) | 0.207 26(3) | 0.636 81(1) | C(21) | −0.184 8(5) | 0.448 9(5) | 0.765 7(2) |
| Fe(1) | 0.256 83(6) | 0.176 07(5) | 0.580 55(2) | C(22) | −0.277 0(5) | 0.412 4(4) | 0.739 9(2) |
| Fe(2) | 0.341 52(4) | 0.310 67(3) | 0.630 39(1) | C(23) | −0.259 7(4) | 0.402 9(4) | 0.703 6(2) |
| P(1) | 0.082 7(1) | 0.507 51(9) | 0.699 14(3) | C(24) | −0.149 5(4) | 0.429 4(4) | 0.692 1(1) |
| P(2) | 0.436 8(1) | 0.277 5(1) | 0.407 00(3) | C(25) | 0.041 4(4) | 0.628 9(3) | 0.682 3(1) |
| O(1) | −0.006 5(4) | 0.533 5(3) | 0.571 3(1) | C(26) | −0.034 9(4) | 0.687 8(4) | 0.700 3(1) |
| O(2) | 0.094 4(4) | 0.305 9(3) | 0.498 41(9) | C(27) | −0.066 4(5) | 0.780 1(4) | 0.686 6(2) |
| O(3) | 0.450 3(4) | 0.469 9(3) | 0.679 5(1) | C(28) | −0.025 2(5) | 0.812 8(4) | 0.655 0(2) |
| O(4) | 0.581 4(3) | 0.225 3(3) | 0.620 6(1) | C(29) | 0.049 9(5) | 0.756 2(4) | 0.636 5(2) |
| O(5) | 0.418 1(4) | 0.212 6(4) | 0.523 4(1) | C(30) | 0.082 9(4) | 0.663 3(4) | 0.650 0(1) |
| O(6) | 0.400 6(4) | 0.013 3(3) | 0.614 8(1) | C(31) | 0.576 1(4) | 0.244 7(4) | 0.436 5(1) |
| O(7) | 0.075 3(3) | 0.059 2(3) | 0.533 3(1) | C(32) | 0.672 3(5) | 0.311 4(4) | 0.440 9(2) |
| O(8) | 0.110 6(4) | −0.006 4(3) | 0.631 7(1) | C(33) | 0.781 5(5) | 0.287 4(5) | 0.463 1(2) |
| O(9) | 0.001 1(4) | 0.218 7(4) | 0.704 1(1) | C(34) | 0.792 9(5) | 0.200 0(5) | 0.481 0(2) |
| O(10) | −0.107 8(3) | 0.229 5(3) | 0.585 2(1) | C(35) | 0.698 2(5) | 0.134 0(5) | 0.477 1(2) |
| O(11) | 0.366 9(3) | 0.444 6(3) | 0.566 0(1) | C(36) | 0.588 0(5) | 0.156 0(4) | 0.454 7(1) |
| O(12) | 0.350 1(3) | 0.173 1(3) | 0.696 02(9) | C(37) | 0.464 8(4) | 0.283 7(3) | 0.358 9(1) |
| C(1) | 0.046 1(5) | 0.462 3(4) | 0.577 5(1) | C(38) | 0.367 6(4) | 0.306 6(4) | 0.331 3(1) |
| C(2) | 0.111 7(4) | 0.315 0(4) | 0.530 1(1) | C(39) | 0.387 0(5) | 0.315 9(4) | 0.294 2(1) |
| C(3) | 0.400 8(4) | 0.409 1(4) | 0.661 7(2) | C(40) | 0.501 8(5) | 0.302 8(4) | 0.284 5(1) |
| C(4) | 0.485 7(4) | 0.256 1(4) | 0.622 9(1) | C(41) | 0.598 4(5) | 0.278 1(5) | 0.311 4(1) |
| C(5) | 0.353 7(5) | 0.200 9(4) | 0.545 6(1) | C(42) | 0.580 3(4) | 0.268 9(4) | 0.348 6(1) |
| C(6) | 0.343 9(4) | 0.078 5(4) | 0.601 6(1) | C(43) | 0.325 2(4) | 0.183 3(3) | 0.410 9(1) |
| C(7) | 0.145 2(4) | 0.105 1(4) | 0.551 5(1) | C(44) | 0.238 0(4) | 0.192 9(4) | 0.435 1(1) |
| C(8) | 0.120 4(5) | 0.076 4(4) | 0.632 2(2) | C(45) | 0.165 3(5) | 0.112 6(4) | 0.440 7(1) |
| C(9) | 0.048 2(5) | 0.220 9(4) | 0.678 1(1) | C(46) | 0.179 0(5) | 0.025 8(4) | 0.422 9(2) |
| C(10) | −0.006 9(4) | 0.246 8(4) | 0.596 8(1) | C(47) | 0.263 4(5) | 0.017 2(4) | 0.398 6(2) |
| C(11) | 0.315 7(4) | 0.393 2(4) | 0.584 5(1) | C(48) | 0.336 6(4) | 0.095 9(4) | 0.392 6(2) |
| C(12) | 0.303 9(5) | 0.210 6(4) | 0.669 3(1) | C(49) | 0.385 6(4) | 0.394 0(3) | 0.422 2(1) |
| C(13) | 0.198 7(4) | 0.523 0(3) | 0.739 8(1) | C(50) | 0.385 3(5) | 0.408 6(4) | 0.460 2(1) |
| C(14) | 0.272 3(5) | 0.445 2(4) | 0.751 4(1) | C(51) | 0.345 1(5) | 0.496 4(4) | 0.473 0(1) |
| C(15) | 0.363 9(5) | 0.453 4(4) | 0.782 5(2) | C(52) | 0.306 6(5) | 0.569 7(4) | 0.448 4(1) |
| C(16) | 0.378 1(5) | 0.540 0(4) | 0.801 4(1) | C(53) | 0.309 4(5) | 0.556 6(4) | 0.410 7(1) |
| C(17) | 0.306 6(5) | 0.618 2(4) | 0.790 0(1) | C(54) | 0.349 3(4) | 0.468 7(4) | 0.397 6(1) |
| C(18) | 0.216 4(4) | 0.610 7(4) | 0.758 9(1) | | | | |

as $[FeRh(CO)_6(\mu-PBu^t_2)]$ [14] or $[(Ph_3P)(OC)_3Fe\{\mu-P(C_6H_{11})_2\}-Rh(CO)(PPh_3)]$,[15] are even more closely related to our compounds since $[Fe(CO)_4]^-$ and $>PR_2$ are isolobal fragments. Indeed, the pattern of intertriangular distances, the square-planar geometry around the rhodium centre, the presence of semibridging CO groups and the spectroscopic data are strikingly similar for **4** and these binuclear compounds.

Two different isomeric metal cages of $[Fe_2Rh_2(CO)_{12}\{Au(PPh_3)\}]^-$ are conceivable; the arrangement with Fe in the apical position is expected to be the most stable, since the number of Au–Rh bonds (presumably stronger than the Au–Fe interactions) is maximized. Accordingly, only this isomer was found in the solid state. The $^{31}P$ NMR spectrum shows only a triplet at $\delta$ 58.6 $[^2J(P–Rh)$ 4.5 Hz], both at room and low temperature, but is not really informative about the structure adopted in solution, since $[Au(PPh_3)]^+$ is usually very mobile.[10,16] The signal can be accounted for either by a static molecule or by a rapid fluxional process of the $[Au(PPh_3)]^+$ group, scrambling over all the inequivalent faces of tetrahedral $[Fe_2Rh_2(CO)_{12}]^{2-}$.

## Experimental

All reactions were carried out under a nitrogen atmosphere, with standard Schlenk-tube techniques.[17] The compounds $[Fe_2(CO)_9]$,[18] $[PPh_4][Rh(CO)_4]$[19] and $[Au(PPh_3)Cl]$[20] were prepared by literature methods. Infrared spectra were recorded with a Perkin-Elmer PC 16 FT-IR spectrophotometer using calcium fluoride cells previously purged with $N_2$, $^{31}P$ NMR spectra on a Bruker AC200 spectrometer operating at 81.0 MHz and reported in ppm downfield from the external standard (85% $H_3PO_4$ in $D_2O$). Elemental analyses were carried out by the Laboratorio di Analisi of the Dipartimento di Chimica Inorganica, Metallorganica e Analitica.

*Preparations.*—$[PPh_4][Fe_2Rh(CO)_9(PPh_3)]$ **4a**. The salt $[PPh_4][Rh(CO)_4]$ (0.45 g, 0.81 mmol) and $[Fe_2(CO)_9]$ (0.30 g, 0.81 mmol) were suspended in tetrahydrofuran (10 cm³) and stirred until all the $[Fe_2(CO)_9]$ had reacted, resulting in a red solution. Solid $PPh_3$ (0.21 g, 0.81 mmol) was added, and the mixture turned deeper red. The solution was then filtered and dried in vacuum. The residue was washed with propanol-2-ol (2 × 5 cm³) and dissolved in thf. This solution was layered with cyclohexane to grow large deep red crystals. Yield 0.50 g, 58% (Found: C, 57.5; H, 2.8. Calc. for $C_{51}H_{35}Fe_2O_9P_2Rh$: C, 57.3; H, 3.3%). $v_{CO}$ in thf at 2020s, 2001w, 1983w, 1966vs, 1948m, 1935m and 1844w (br) cm⁻¹. $\delta_P$ 21.9 (1 P, s, $[PPh_4]^+$) and 29.2 [1 P, d, $^1J(P–Rh)$ 170.4 Hz, $PPh_3$].[15,21]

$[N(PPh_3)_2]_2[Fe_2Rh_2(CO)_{12}]$ **1a**. The salt $[N(PPh_3)_2][Rh(CO)_4]$ (0.45 g, 0.53 mmol) and $[Fe_2(CO)_9]$ (0.10 g, 0.27 mmol) were suspended in acetone (20 cm³) and refluxed for 2 h. The completeness of the reaction was checked by infrared spectroscopy, and the solution was filtered. Propan-2-ol was carefully layered on top and well shaped crystals were formed. Yield 0.39 g, 83% (Found: C, 58.2; H, 4.2; N, 1.8. Calc. for $C_{84}H_{60}Fe_2N_2O_{12}P_4Rh_2$: C, 58.2; H, 3.5; N, 1.6%). Selected crystals of compound **1a** in MeCN showed infrared bands at 2016w, 1967s, 1947vs, 1903m, 1800m and 1768s cm⁻¹.

$[PPh_4]_2[Fe_2Rh_2(CO)_{12}]$ **1b**. The $[PPh_4]^+$ salt was similarly obtained by using $[PPh_4][Rh(CO)_4]$. After 2 h of reaction, the solution was filtered, the solvent removed in vacuum, and the residue stirred with MeOH (15 cm³) for 2 h. The product was

filtered off and found to be sufficiently pure (IR spectrum) for synthetic purposes. Crystals of compound **1b** were grown from acetone–propan-2-ol or MeCN–diisopropyl ether.

Both salts **1a** and **1b** are very soluble in acetone and acetonitrile, poorly soluble in thf and insoluble in alcohols.

[PPh$_4$][Fe$_2$Rh$_2$(CO)$_{12}$\{Au(PPh$_3$)\}] **2a**. The salt [PPh$_4$]$_2$-[Fe$_2$Rh$_2$(CO)$_{12}$] (0.13 g; 0.097 mmol) and [Au(PPh$_3$)Cl] (0.05 g; 0.097 mmol) were dissolved in acetone (10 cm$^3$) and stirred for 30 min, during which time the solution turned red-brown. Propanol-2-ol (10 cm$^3$) was then added to the stirred solution and the solvent volume was reduced under vacuum to about one half, to ensure precipitation. The dark brown flaky residue was filtered off, washed with propanol-2-ol (2 × 5 cm$^3$) and dried in vacuum. It was then dissolved in thf (6 cm$^3$) and layered with cyclohexane. Yield 0.092 g, 65% (Found: C, 45.0; H, 2.2. Calc. for C$_{54}$H$_{35}$AuFe$_2$O$_{12}$P$_2$Rh$_2$: C, 44.7; H, 2.4%). $\nu_{CO}$ in thf at 2056vw, 2033m, 1979vs, 1964s, 1921m, 1839w and 1806m cm$^{-1}$. $\delta_P$ 21.9 (1 P, s, [PPh$_4$]$^+$) and 58.6 [1 P, t, $^2J$(P–Rh) 4.5 Hz]; this coupling constant can be compared to those reported for [Rh$_6$C(CO)$_{13}$Au$_2$(PPh$_3$)$_2$] (3.8 Hz) and [Rh$_6$C(CO)$_{15}$\{Au(PPh$_3$)\}$_2$] (5.0 Hz).[16] The spectrum is invariant at 193 K.

*X-Ray Crystallography for Compounds* **4a** *and* **2a**.—Crystal data and other experimental details are summarized in Table 3. The diffraction experiments were carried out on an Enraf-Nonius CAD-4 diffractometer at room temperature using Mo-K$\alpha$ radiation ($\lambda = 0.710\,73$ Å) with a graphite-crystal monochromator in the incident beam. The calculations were performed on a PDP 11/73 computer using the SDP package and the physical constants tabulated therein.[22] A periodic monitoring of three standard reflections revealed a crystal decay, *ca.* 2.7% for **4a** and 5.5% for **2a** (on intensities) at the end of data collection. The diffracted intensities were corrected for Lorentz, polarization, decay and absorption effects (empirical).[23] Scattering factors and anomalous dispersion corrections were taken from ref. 24. The structures were solved by MULTAN[25] and Fourier-difference syntheses and refined by full-matrix least squares, minimizing the function $\Sigma w(F_o - k|F_c|)^2$. Anisotropic thermal factors were refined for all the non-hydrogen atoms. Hydrogen atoms were placed in their ideal positions (C–H 0.97 Å, $B = 1.20$ times that of the carbon atom to which they are attached) and not refined. For compound **2a** the atoms Rh(2) and Fe(2) showed, in the first stages of refinement, anomalous thermal parameters, which suggested the presence of rhodium–iron substitutional disorder. Refinement of the occupancy factors led to metal distributions of Rh$_{0.56}$Fe$_{0.44}$ for the Rh(2) site and of Rh$_{0.44}$Fe$_{0.56}$ for the Fe(2) site. The final Fourier maps showed maximum residuals of 0.26(4) e Å$^{-3}$ at 1.01 Å from rhodium for compound **4a**, and of 0.72(7) e Å$^{-3}$ at 1.09 Å from the gold atom for **2a**. The atomic coordinates are listed in Tables 4 and 5, respectively.

Additional material available from the Cambridge Crystallographic Data Centre comprises H-atom coordinates, thermal parameters and remaining bond lengths and angles.

## Acknowledgements

## References

1 A. Ceriotti, G. Longoni, R. Della Pergola, B. T. Heaton and D. O. Smith, *J. Chem. Soc., Dalton Trans.*, 1983, 1433.
2 A. Ceriotti, R. Della Pergola, G. Longoni, B. T. Heaton, F. Demartin and M. Manassero, *J. Organomet. Chem.*, 1986, **311**, C31.
3 R. Della Pergola, L. Garlaschelli, F. Demartin, M. Manassero, N. Masciocchi and G. Longoni, *J. Organomet. Chem.*, 1988, **352**, C59.
4 R. Della Pergola, L. Garlaschelli, F. Demartin, M. Manassero, N. Masciocchi and M. Sansoni, *J. Chem. Soc., Dalton Trans.*, 1990, 127.
5 R. Della Pergola, A. Ceriotti, L. Garlaschelli, F. Demartin, M. Manassero and N. Masciocchi, *Inorg. Chem.*, 1993, **32**, 3349.
6 R. Psaro, C. Dossi, R. Della Pergola, L. Garlaschelli, S. Calmotti, S. Marengo, M. Bellatreccia and R. Zanoni, *Appl. Catal. A Gen.*, 1995, **121**, L19.
7 H. H. Ohst and J. K. Kochi, *Organometallics*, 1986, **5**, 1359; G. B. Jacobsen, B. L. Shaw and M. Thornton-Pett, *J. Chem. Soc., Dalton Trans.*, 1987, 2751; H. Bantel, A. K. Powell and H. Varenkamp, *Chem. Ber.*, 1990, **123**, 677.
8 ORTEP, A Fortran thermal-ellipsoid program for crystal structure illustration, C. K. Johnson, Oak Ridge National Laboratory, Oak Ridge, TN, 1971.
9 M. Tachikawa, A. C. Sievert, E. L. Mutterties, M. R. Thompson, C. S. Day and V. W. Day, *J. Am. Chem. Soc.*, 1980, **102**, 1725.
10 C. E. Housecroft, D. M. Matthews, A. Waller, A. J. Edwards and A. L. Rheingold, *J. Chem. Soc., Dalton Trans.*, 1993, 3059; A. Ceriotti, R. Della Pergola, L. Garlaschelli, M. Manassero and N. Masciocchi, *Organometallics*, 1995, **14**, 186.
11 S. M. Owen, *Polyhedron*, 1988, **7**, 253.
12 M. R. Churchill and B. G. DeBoer, *Inorg. Chem.*, 1977, **16**, 2397; A. G. Orpen, A. V. Rivera, E. G. Bryan, D. Pippard, G. M. Sheldrick and K. D. Rouse, *J. Chem. Soc., Chem. Commun.*, 1978, 723.
13 C. Mealli, *J. Am. Chem. Soc.*, 1985, **107**, 2245 and refs. therein; L. J. Farrugia, *Adv. Organomet. Chem.*, 1990, **31**, 301.
14 H. Hartung, A. Krug and H.-C. Böttcher, *J. Organomet. Chem.*, 1995, **487**, C1.
15 H. A. Jenkins, S. J. Loeb and D. W. Stephan, *Inorg. Chem.*, 1989, **28**, 1998.
16 A. Fumagalli, S. Martinengo, V. G. Albano, D. Braga and F. Grepioni, *J. Chem. Soc., Dalton Trans.*, 1989, 2343.
17 D. F. Shriver and M. A. Drezdzon, *The Manipulation of Air-sensitive Compounds*, 2nd edn., Wiley, New York, 1986.
18 E. H. Braye and W. Hübel, *Inorg. Synth.*, 1966, **8**, 178.
19 R. Della Pergola, L. Garlaschelli and S. Martinengo, *Inorg. Synth.*, 1991, **28**, 178.
20 M. I. Bruce, B. K. Nicholson and O. Bin Shawkataly, *Inorg. Synth.*, 1989, **26**, 324.
21 L. J. Farrugia, A. D. Miles and F. G. A. Stone, *J. Chem. Soc., Dalton Trans.*, 1984, 2415 and refs. therein.
22 B. A. Frenz and Associates, SDP Plus Version 1.0, Enraf-Nonius, Delft, 1980.
23 A. C. T. North, D. C. Phillips and F. S. Mathews, *Acta Crystallogr., Sect. A*, 1968, **24**, 351.
24 *International Tables for X-Ray Crystallography*, Kynoch Press, Birmingham, 1974, vol. 4.
25 P. Main, S. J. Fiske, S. E. Hill, L. Lessinger, G. Germain, J. P. Declercq and M. M. Wolfson, MULTAN 80, A system of computer programs for the automatic solution of crystal structures from X-ray diffraction data, Universities of York and Louvain, 1980.